The Backscattered Fraction in Two-Stream Approximations

W. J. WISCOMBE AND G. W. GRAMS

National Center for Atmospheric Research[1], *Boulder, Colo. 80307*

(Manuscript received 2 March 1976, in revised form 13 August 1976)

ABSTRACT

New formulas for the backscattered fraction in two-stream theory are derived. They express this fraction, for either isotropically or monodirectionally incident radiation, as a single integral over the scattering phase function, thereby effecting a substantial simplification over the customary multiple-integral definitions. From these formulas the globally averaged backscatter of the earth due to typical aerosols is shown to depend primarily on the *forward* part (0° to 90°) of the scattering phase function, where the disagreement between spherical- and nonspherical-particle scattering is smallest. The new formulas also lead to connections, in terms of standard elliptic integrals, between the backscatter and the phase function asymmetry factor; while rigorously correct only for the Henyey-Greenstein phase function, these relations are shown to be remarkably accurate for *all* spherical-particle phase functions. The detailed relationship between backscatter and asymmetry factor is shown to be multi-valued; thus two-stream and Eddington approximations cannot be uniquely related.

The common approximation of the globally averaged backscatter, or Bond albedo, by the backscatter for radiation incident at solar zenith angles of 0° or 60° is shown to lead, for a wide range of particle sizes and optical properties, to systematic and often large underestimates. The solar-spectrum-integrated enhancement of the Bond albedo due to a uniform, optically thin aerosol layer is examined, holding the total mass of aerosol fixed and varying the particle radii and optical properties over wide ranges. The particle radius at which maximum albedo enhancement occurs decreases from 0.3 μm down to about 0.08 μm as the particle absorptivity increases. Also, increasing the absorption of particles smaller than 0.1 μm actually raises the albedo in contrast to the usual situation where absorption suppresses backscattering.

1. Introduction

The azimuthally integrated, plane-parallel, radiative transfer equation has the following form for wavelengths in the solar spectrum:

$$\mu\frac{\partial I}{\partial\tau}+I=\frac{\omega S_0}{4\pi}\bar{P}(\mu,\mu_0)e^{-\tau/\mu_0}+\frac{\omega}{2}\int_{-1}^{1}\bar{P}(\mu,\mu')I(\tau,\mu')d\mu'. \quad (1)$$

Here I is the azimuthally averaged diffuse intensity, μ the cosine of the angle measured from the downward normal, τ the optical depth, ω the single-scattering albedo and μ_0 the cosine of the zenith angle at which the monodirectional flux S_0 is incident (at $\tau=0$). The azimuthally integrated phase function $\bar{P}$ is

$$\bar{P}(\mu,\mu')\equiv\frac{1}{\pi}\int_0^{\pi}P(\mu\mu'+(1-\mu^2)^{\frac{1}{2}}(1-\mu'^2)^{\frac{1}{2}}\cos\phi)d\phi, \quad (2)$$

where P is the usual scattering phase function, normalized to unity:

$$\frac{1}{2}\int_0^{\pi}P(\cos\theta)\sin\theta\,d\theta=1, \quad (3a)$$

$$\frac{1}{2}\int_{-1}^{1}\bar{P}(\mu,\mu')d\mu'=1. \quad (3b)$$

Eqs. (3a) and (3b) are equivalent.

The Schuster–Schwarzschild two-stream (SSTS) approximation assumes I to be hemispherically isotropic, i.e.,

$$I=\begin{cases}I^+(\tau), & \mu>0\\ I^-(\tau), & \mu<0\end{cases}$$

which leads, after integration of Eq. (1) over $\mu\in[0,1]$ and $\mu\in[-1,0]$, to

$$\frac{1}{2}\frac{dI^+}{d\tau}=-(1-\omega)I^+-\omega\bar{\beta}(I^+-I^-)+\frac{\omega S_0}{2\pi}[1-\beta(\mu_0)]e^{-\tau/\mu_0}, \quad (4a)$$

$$\frac{1}{2}\frac{dI^-}{d\tau}=(1-\omega)I^--\omega\bar{\beta}(I^+-I^-)-\frac{\omega S_0}{2\pi}\beta(\mu_0)e^{-\tau/\mu_0}, \quad (4b)$$

[1] The National Center for Atmospheric Research is sponsored by the National Science Foundation.

The Backscattered Fraction in Two-Stream Approximations

W. J. WISCOMBE AND G. W. GRAMS

National Center for Atmospheric Research[1], *Boulder, Colo. 80307*

(Manuscript received 2 March 1976, in revised form 13 August 1976)

ABSTRACT

New formulas for the backscattered fraction in two-stream theory are derived. They express this fraction, for either isotropically or monodirectionally incident radiation, as a single integral over the scattering phase function, thereby effecting a substantial simplification over the customary multiple-integral definitions. From these formulas the globally averaged backscatter of the earth due to typical aerosols is shown to depend primarily on the *forward* part (0° to 90°) of the scattering phase function, where the disagreement between spherical- and nonspherical-particle scattering is smallest. The new formulas also lead to connections, in terms of standard elliptic integrals, between the backscatter and the phase function asymmetry factor; while rigorously correct only for the Henyey-Greenstein phase function, these relations are shown to be remarkably accurate for *all* spherical-particle phase functions. The detailed relationship between backscatter and asymmetry factor is shown to be multi-valued; thus two-stream and Eddington approximations cannot be uniquely related.

The common approximation of the globally averaged backscatter, or Bond albedo, by the backscatter for radiation incident at solar zenith angles of 0° or 60° is shown to lead, for a wide range of particle sizes and optical properties, to systematic and often large underestimates. The solar-spectrum-integrated enhancement of the Bond albedo due to a uniform, optically thin aerosol layer is examined, holding the total mass of aerosol fixed and varying the particle radii and optical properties over wide ranges. The particle radius at which maximum albedo enhancement occurs decreases from 0.3 μm down to about 0.08 μm as the particle absorptivity increases. Also, increasing the absorption of particles smaller than 0.1 μm actually raises the albedo in contrast to the usual situation where absorption suppresses backscattering.

1. Introduction

The azimuthally integrated, plane-parallel, radiative transfer equation has the following form for wavelengths in the solar spectrum:

$$\mu\frac{\partial I}{\partial\tau}+I=\frac{\omega S_0}{4\pi}\tilde{P}(\mu,\mu_0)e^{-\tau/\mu_0}+\frac{\omega}{2}\int_{-1}^{1}\tilde{P}(\mu,\mu')I(\tau,\mu')d\mu'. \quad (1)$$

Here I is the azimuthally averaged diffuse intensity, μ the cosine of the angle measured from the downward normal, τ the optical depth, ω the single-scattering albedo and μ_0 the cosine of the zenith angle at which the monodirectional flux S_0 is incident (at $\tau=0$). The azimuthally integrated phase function $\tilde{P}$ is

$$\tilde{P}(\mu,\mu')\equiv\frac{1}{\pi}\int_0^{\pi}P(\mu\mu'+(1-\mu^2)^{\frac{1}{2}}(1-\mu'^2)^{\frac{1}{2}}\cos\phi)d\phi, \quad (2)$$

where P is the usual scattering phase function, normalized to unity:

$$\frac{1}{2}\int_0^{\pi}P(\cos\theta)\sin\theta\,d\theta=1, \quad (3a)$$

$$\frac{1}{2}\int_{-1}^{1}\tilde{P}(\mu,\mu')d\mu'=1. \quad (3b)$$

Eqs. (3a) and (3b) are equivalent.

The Schuster–Schwarzschild two-stream (SSTS) approximation assumes I to be hemispherically isotropic, i.e.,

$$I=\begin{cases}I^+(\tau), & \mu>0\\ I^-(\tau), & \mu<0\end{cases}$$

which leads, after integration of Eq. (1) over $\mu\in[0,1]$ and $\mu\in[-1,0]$, to

$$\frac{1}{2}\frac{dI^+}{d\tau}=-(1-\omega)I^+-\omega\tilde{\beta}(I^+-I^-)+\frac{\omega S_0}{2\pi}[1-\beta(\mu_0)]e^{-\tau/\mu_0}, \quad (4a)$$

$$\frac{1}{2}\frac{dI^-}{d\tau}=(1-\omega)I^--\omega\tilde{\beta}(I^+-I^-)-\frac{\omega S_0}{2\pi}\beta(\mu_0)e^{-\tau/\mu_0}, \quad (4b)$$

[1] The National Center for Atmospheric Research is sponsored by the National Science Foundation.

where β is the backscattered fraction for monodirectional radiation incident at zenith angle $\theta_0 = \cos^{-1}\mu_0$,

$$\beta(\mu_0) \equiv \frac{1}{2}\int_0^1 \bar{P}(-\mu', \mu_0)d\mu', \tag{5}$$

and $\bar{\beta}$ is the backscattered fraction for isotropically incident radiation,

$$\bar{\beta} \equiv \int_0^1 \beta(\mu)d\mu. \tag{6}$$

Coakley and Chýlek (1975) give a fuller discussion. $\bar{\beta}$ is, of course, related to the spherical or Bond albedo of a planet illuminated by monodirectional radiation. Note that $\bar{\beta}$ and $\beta(\mu_0)$ are, respectively, triple and double integrals over the scattering phase function P. Below we shall reduce them both to single integrals.

A second two-stream approximation, based on the discrete ordinate method (Chandrasekhar, 1960; Liou, 1973), leads to a backscattered fraction of

$$\beta_c = \tfrac{1}{2}\bar{P}(1/\sqrt{3}, -1/\sqrt{3})$$

(cf. Lyzenga, 1973). This has been used in applications primarily in the modified form of Sagan and Pollack (1967), who assumed

$$\beta_c \approx \tfrac{1}{2}(1-g), \tag{7}$$

where g is the phase function asymmetry factor

$$g \equiv \frac{1}{2}\int_0^\pi \cos\theta P(\cos\theta)\sin\theta d\theta. \tag{8}$$

The Sagan–Pollack two-stream equations are similar to Eqs. (4a, b), except that a mean angle cosine of $1/\sqrt{3}$ is used on the left-hand sides in place of $\frac{1}{2}$, and $\frac{1}{2}(1-g)$ replaces $\bar{\beta}$. Since a formulation of the SSTS approximation in terms of g may be advantageous in some circumstances, and for other reasons as well, the relation between $\bar{\beta}$ and g is explored below in some detail.

For a scattering layer of optical thickness $\Delta\tau \ll 1$—for example for a typical stratospheric aerosol—the albedo for monodirectionally incident radiation is

$$R(\mu) = \omega\beta(\mu)\frac{\Delta\tau}{\mu}, \tag{9}$$

and for isotropically incident radiation

$$\bar{R} = 2\omega\bar{\beta}\Delta\tau \tag{10}$$

which is also the Bond albedo. Eqs. (9) and (10) proceed rigorously from Eq. (1) in the limit $\tau \to 0$ (Coakley and Chýlek, 1975). Since

$$R(\tfrac{1}{2}) = 2\omega\beta(\tfrac{1}{2})\Delta\tau,$$

the genesis of the "60° mean zenith angle approximation," in which $R(\frac{1}{2})$ is used for $\bar{R}$ or $\beta(\frac{1}{2})$ is used for $\bar{\beta}$, is apparent. We evaluate this approximation below, as well as the equally common substitution (at least in climate modeling) of $\beta(1)$ for $\bar{\beta}$.

All of the quantities $\beta(\mu_0)$, $\bar{\beta}$, β_c, $R(\mu_0)$ and $\bar{R}$ defined above have at one time or another been called the "backscatter." Such a multiplicity of definitions is likely to leave the casual user of two-stream approximations somewhat confused, and this confusion can only be abetted by theoretical papers which do not define "backscatter" in precise mathematical terms. The situation has been further worsened by the frequently cited paper of Irvine (1968), in which $\beta(1)$ is mistakenly used in the SSTS approximation, although Irvine was merely propagating an error committed originally by Chu and Churchill (1955). In Table 1 we have indicated a number of papers, dating back to 1921, which have employed two-stream approximations in meteorological applications. In each case the particular "backscatter" used, and where feasible a value or range of values, is given. The diversity of definitions of "backscatter" is apparent, although actual values tend to be concentrated in the range 0.1–0.2. Table 1 also shows an excessive reliance on Mie calculations, occasioned by the dearth of actual measurements of scattering phase functions and backscattering. Finally, it shows a resurgence of interest in two-stream methods in the last decade, stemming primarily from a need for simple analytic estimates of aerosol effects on the radiation budget. One such study (for stratospheric aerosols) led to the results in this paper.

2. Formula for $\bar{\beta}$ and discussion

If we expand the phase function in Legendre polynomials P_n, viz.

$$P(\mu) = \sum_{n=0}^{\infty} \omega_n P_n(\mu),$$

then the addition theorem for spherical harmonics and Eq. (2) lead to

$$\bar{P}(\mu,\mu') = \sum_{n=0}^{\infty} \omega_n P_n(\mu)P_n(\mu'). \tag{11}$$

Because of Eq. (3a), $\omega_0 = 1$. Using Eq. (11) in Eqs. (5) and (6) and switching sum and integration give

$$\bar{\beta} = \tfrac{1}{2}\sum_{n=0}^{\infty} \omega_n \int_0^1 P_n(\mu)d\mu \int_0^1 P_n(-\mu')d\mu'.$$

The second integral, according to the relation $P_n(-\mu) = (-1)^n P_n(\mu)$, is proportional to the first one, and the first integral is given in standard references, which leads to

$$\bar{\beta} = \frac{1}{2} - \frac{1}{8}\sum_{m=0}^{\infty} \left[\frac{\Gamma(m+\frac{1}{2})}{\Gamma(m+2)}\right]^2 \omega_{2m+1}. \tag{12}$$

TABLE 1. Meteorological chronology of the use of the "backscatter" concept.

Author(s)	"Backscatter"	Source
Mecke (1921)	$\beta(1)=0.0725$	Geometric optics calculation, water drop
Dietzius (1922)	$\beta(\theta)$ for $\theta=0°$, 10° ..., 90°; $\bar{\beta}=\beta(67°)=0.195$	Same as Mecke (1921)
Albrecht (1933)	$\omega_1\beta(\mu)+\omega_2\bar{\beta}$ (ω_1= direct fraction, ω_2 = diffuse fraction)	Dietzius (1922)
Hewson (1943)	$\bar{\beta}=\beta(67°)=0.195$	Dietzius (1922)
Roach (1961)	Average $\beta(\mu)=0.0625$	Field measurement (lowest 1000 ft)
Robinson (1963)	$\beta(\mu)$ for $\mu=0.2$, 0.3, ..., 1.0	Deduced from Waldram's phase function measurements
Lettau and Lettau (1969)	$\bar{\beta}=\begin{cases}\frac{1}{3} & \uparrow\text{space}\\ 0.05\text{–}0.2 & \downarrow\text{ground}\end{cases}$	Estimated from measurements for entire atmospheric column
Charlson and Pilat (1969)	$\beta(1)\approx 0.1$	Deduced from Bullrich's phase functions
Atwater (1970)	$\frac{1}{3}$	Lettau and Lettau (1969)
Rasool and Schneider (1971)	$\beta_c=0.18$	Sagan-Pollack approximation, using Mie theory for g at $\lambda=0.55$ μm
Ensor *et al.* (1971)	$\beta(1)$ (as "efficiency factor"; no values given)	Mie theory
Barrett (1971)	$\beta(1)=0.175$	Mie theory
Mitchell (1971)	$R(\mu)=0$–0.02	Assumed range
Schneider (1971)	$R(\mu)=0.01-0.10$	Assumed range
Neumann and Cohen (1972)	$R(\mu)=0-0.20$	Assumed range
Sellers (1973)	$\beta_c=\begin{cases}0.18 & \text{clear}\\ 0.08 & \text{cloudy}\end{cases}$	Sagan-Pollack approximation (values refer to entire atmospheric column)
Chýlek and Coakley (1974)	$\bar{\beta}=0.1$	Assumed
Charlson *et al.* (1974)	$\beta(1)=0.1-0.2$	Nephelometer measurement
Cadle and Grams (1975)	$\bar{\beta}$, $\beta(\frac{1}{2})$, $\beta(1)$ (as "efficiency factors")	Mie theory
Russell and Grams (1975)	$\beta(1)$ (no values given)	Mie theory
Chýlek *et al.* (1975)	$\beta(1)$ (as "efficiency factor") and $R(1)$ for whole solar spectrum	Mie theory
Joseph and Wolfson (1975)	$\beta(\mu)$	Robinson (1963)

But since the expansion coefficients ω_n are given by

$$\omega_n=\tfrac{1}{2}(2n+1)\int_{-1}^{1}P(\mu)P_n(\mu)d\mu, \tag{13}$$

we may substitute this expression into Eq. (12) and again switch sum and integration to yield

$$\bar{\beta}=\frac{1}{2}-\frac{1}{4}\int_{-1}^{1}S(\mu)P(\mu)d\mu, \tag{14}$$

where

$$S(\mu)\equiv(2\pi)^{-1}\sum_{m=0}^{\infty}(2m+\tfrac{3}{2})\left[\frac{\Gamma(m+\frac{1}{2})}{\Gamma(m+2)}\right]^2P_{2m+1}(\mu).$$

From Mangulis (1965, p. 125), this last series has a closed-form sum,

$$S(\mu)=1-\frac{2}{\pi}\cos^{-1}\mu,$$

which, when inserted back into Eq. (14), leads to

$$\bar{\beta}=(2\pi)^{-1}\int_{-1}^{1}\cos^{-1}\mu P(\mu)d\mu \tag{15a}$$

$$=(2\pi)^{-1}\int_{0}^{\pi}\theta P(\cos\theta)\sin\theta d\theta. \tag{15b}$$

The phase function normalization condition (3a) has been used to simplify this result. Eq. (15) gives a simple representation of $\bar{\beta}$ as a single integral over the phase function.

The derivative of the integrand in the form (15a) is infinite at $\mu=\pm 1$, hence the form (15b) is preferable if numerical quadrature is to be used to compute $\bar{\beta}$. This is because standard quadrature rules, being adapted to polynomials, are very inaccurate when applied to functions with cusps (see, e.g., Davis and Rabinowitz, 1967).

Hansen (1969) has shown that the Henyey–Greenstein phase function

$$P_{\mathrm{HG}}(\mu)\equiv\frac{1-g^2}{(1+g^2-2g\mu)^{\frac{3}{2}}} \tag{16}$$

(where g is the asymmetry factor) can be used to replace the more realistic Mie phase functions in multiple scattering calculations, with no more than a few percent error in computed fluxes. For $P=P_{\mathrm{HG}}$, Eq. (15) leads to

$$\bar{\beta}_{\mathrm{HG}}=\frac{1-g}{2g}\left[\frac{2}{\pi}(1+g)K(g^2)-1\right], \tag{17}$$

where K is the complete elliptic integral of the first kind:

$$K(g^2)\equiv\int_{0}^{\pi/2}(1-g^2\sin^2\theta)^{-\frac{1}{2}}d\theta.$$

Plots of $\bar{\beta}_{\mathrm{HG}}$ will be given in Fig. 3 and again in Section 4, where $\bar{\beta}_{\mathrm{HG}}$ is shown to be an excellent approximation to the value of $\bar{\beta}$ for spherical particles.

We note from Eq. (15) that the full angular range of the phase function, 0° to 180°, contributes to $\bar{\beta}$. This is in sharp contrast to $\beta(1)$, which has been used in some meteorological applications (see Table 1) and which is merely the integral of the phase function from 90° to 180° [see Eq. (23)]. We have found that across most of the solar spectrum, phase function values between 0° and 90° contribute at least 70% of the entire value of $\bar{\beta}$. This is extremely important *vis à vis* the effects of non-sphericity on $\bar{\beta}$, for experiments (Holland and Gagne, 1970; Chýlek *et al.*, 1976) indicate that the primary differences between Mie phase functions and measured ones for non-spherical aerosols are in the range 90° to 180°. Our result shows that these differences have reduced leverage to alter $\bar{\beta}$, since at most 30% of $\bar{\beta}$ is associated with the 90° to 180° range of angles. Thus the effect of non-sphericity on the globally averaged backscattering, as represented by $\bar{\beta}$, may not be nearly as large as some have thought.

In order to illustrate the point discussed in the preceding paragraph, we have plotted in Fig. 1 the integrand $[\theta\sin\theta P(\cos\theta)]$ of Eq. (15) versus θ, for several phase functions $P(\cos\theta)$. The total area under each curve is proportional to $\bar{\beta}$, and in each case we have indicated the fraction of that area associated with the 0°–90° and 90°–180° angular ranges. Figs. 1a and 1b refer to Henyey–Greenstein phase functions (16) with $g=0.7$ and $g=0.9$, respectively. (These particular values of g fairly well delimit the variation for aerosols and clouds.) Note that the forward hemisphere of the phase function accounts for 74% and 85%, respectively, of the value of $\bar{\beta}$ in these two cases. Figs. 1c and 1d refer to Mie theory phase functions at a wavelength of 0.5 μm for ensembles of scattering particles with power-law size distributions $n(r)\propto r^{-\alpha}$ (Junge, 1963). Integrals were calculated over the particle-radius interval from 0.01 to 10 μm for $\alpha=4$ in Fig. 1c and $\alpha=2$ in Fig. 1d for a refractive index of $1.5-0.02i$. These particular specifications are not unrepresentative of some atmospheric aerosols, and they give values of g roughly the same as for the two Henyey–Greenstein cases (Figs. 1a and 1b). The forward hemisphere of the phase function accounts for 71% and 72%, respectively, of the value of $\bar{\beta}$ in Figs. 1c and 1d. These percentages are smaller than in the corresponding Henyey–Greenstein cases, and furthermore do not increase significantly as g increases. This is because Mie theory phase functions are not monotonic like Henyey–Greenstein ones but have secondary peaks in the 90°–180° region, which are visible in Figs. 1c and 1d; and also because Mie theory phase functions have a larger percentage of their area associated with very small angles where the factor $\theta\sin\theta$ substantially reduces the integrand.

3. Formula for $\beta(\mu)$ and discussion

We proceed as we did for $\bar{\beta}$, replacing $\bar{P}$ in Eq. (5) by its Legendre polynomial expansion (11), switching sum and integral, and using the same Legendre polynomial integral as before to yield the series expansion

$$\beta(\mu)=\frac{1}{2}-\frac{1}{4\pi^{\frac{1}{2}}}\sum_{m=0}^{\infty}(-1)^m\frac{\Gamma(m+\frac{1}{2})}{\Gamma(m+2)}\omega_{2m+1}P_{2m+1}(\mu).$$

If we now insert the definition (13) of the expansion coefficient ω_n, and again switch sum and integral, we

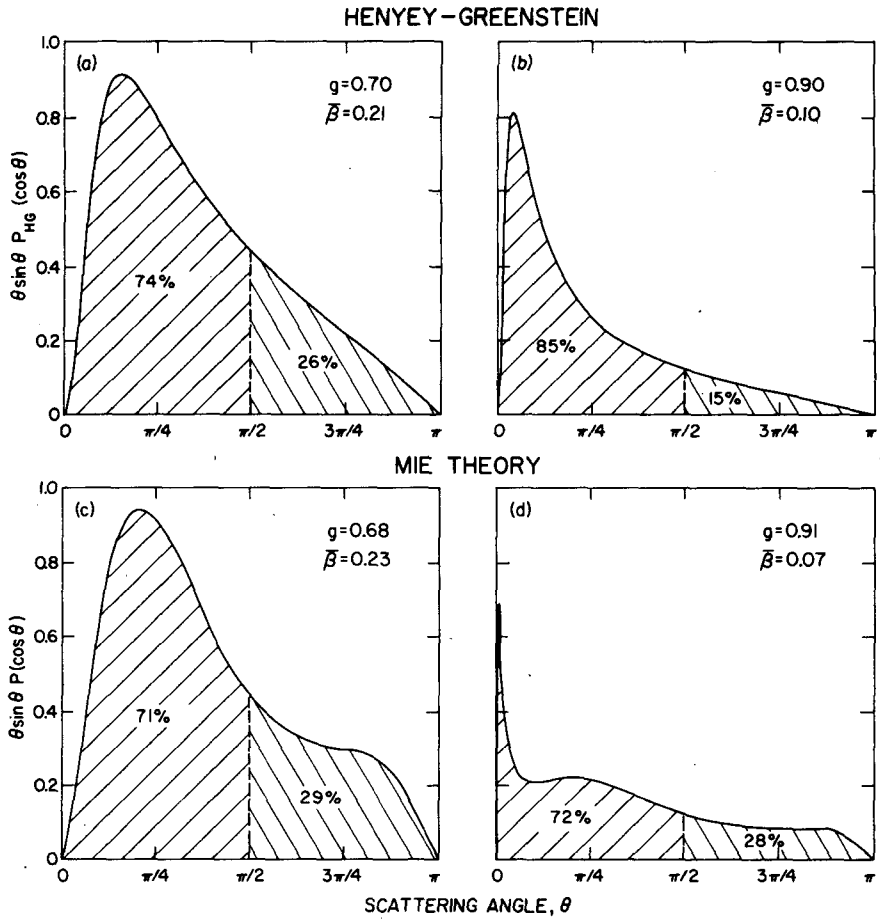

FIG. 1. Plots of $\theta \sin\theta\, P(\cos\theta)$ versus θ for various phase functions $P(\cos\theta)$. Fractions of the area under each curve due to $\theta\in[0°, 90°]$ and $\theta\in[90°, 180°]$ are indicated. Cases (a) and (b) are for Henyey–Greenstein phase functions with $g=0.7$ and $g=0.9$. Cases (c) and (d) are for Mie theory phase functions at 0.5 μm wavelength, 1.5–0.02i index of refraction, and r^{-4} and r^{-2} size distributions for the radius interval 0.01 μm$<r<$10 μm.

arrive at

$$\beta(\mu)=\frac{1}{2}-\frac{1}{4}\int_{-1}^{1} A(\mu,\mu')P(\mu')d\mu', \tag{18}$$

where

$$A(\mu,\mu')\equiv\frac{1}{\pi^{\frac{1}{2}}}\sum_{m=0}^{\infty}(-1)^m(2m+\tfrac{3}{2}) \times\frac{\Gamma(m+\frac{1}{2})}{\Gamma(m+2)}P_{2m+1}(\mu)P_{2m+1}(\mu'). \tag{19}$$

When confronted with a product of Legendre polynomials with different arguments, such as in the last sum, it is often helpful to use an addition theorem to replace the product by a single Legendre polynomial with a more complex argument. The following such relation proves useful in the present case:

$$P_n(\mu)P_n(\mu') =\pi^{-1}\int_0^{\pi} P_n[\mu\mu'+(1-\mu^2)^{\frac{1}{2}}(1-\mu'^2)^{\frac{1}{2}}\cos\phi]d\phi.$$

Putting this into Eq. (19) leads to

$$A(\mu,\mu') =\pi^{-1}\int_0^{\pi} Q[\mu\mu'+(1-\mu^2)^{\frac{1}{2}}(1-\mu'^2)^{\frac{1}{2}}\cos\phi]d\phi, \tag{20}$$

where

$$Q(\mu)\equiv\frac{1}{\pi^{\frac{1}{2}}}\sum_{m=0}^{\infty}(-1)^m(2m+\tfrac{3}{2})\frac{\Gamma(m+\frac{1}{2})}{\Gamma(m+2)}P_{2m+1}(\mu).$$

From Mangulis (1965, p. 125), $Q(\mu)$ is simply a step function,

$$Q(\mu)=\begin{cases}-1, & -1\leqslant\mu\leqslant 0\\ +1, & 0<\mu\leqslant 1.\end{cases}$$

Thus the integral over Q in Eq. (20) is trivial. The only complication is that the step, which occurs when the argument of Q vanishes,

$$\cos\theta\cos\theta'+\sin\theta\sin\theta'\cos\phi_0=0$$

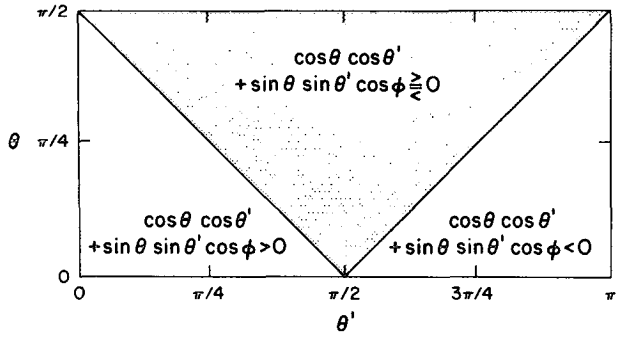

FIG. 2. The θ-θ' plane; the stippled region satisfies condition (21). In the other two regions the argument of Q in Eq. (20) is strictly positive or strictly negative for $\phi\in[0,\pi]$ as indicated.

or

$$\phi_0=\cos^{-1}(-\mathrm{ctn}\theta\ \mathrm{ctn}\theta')=\pi-\cos^{-1}(\mathrm{ctn}\theta\ \mathrm{ctn}\theta')$$

will only occur for $\phi_0\in[0,\pi]$ (the integration interval) if

$$-1\leqslant\mathrm{ctn}\theta\ \mathrm{ctn}\theta'\leqslant 1. \tag{21}$$

The region of the θ-θ' plane for which this condition is satisfied is stippled in Fig. 2. It is bounded by the three straight lines $\theta=\pi/2$, $\theta'=\pi/2-\theta$ and $\theta'=\pi/2+\theta$; within it Eq. (20) becomes

$$A(\mu,\mu')=\pi^{-1}\left\{\int_0^{\phi_0}(+1)d\phi+\int_{\phi_0}^{\pi}(-1)d\phi\right\}=2\pi^{-1}\phi_0-1.$$

Outside the stippled region, Q in Eq. (20) is always either $+1$ or -1 (for the left-most or right-most regions, respectively, in Fig. 2), so that A is also either $+1$ or -1, independent of θ and θ'. Summing up, we have

$$A(\mu,\mu')=\begin{cases}+1, & 0\leqslant\theta'\leqslant\dfrac{\pi}{2}-\theta\\ 1-2\pi^{-1}\cos^{-1}(\mathrm{ctn}\theta\ \mathrm{ctn}\theta'), & \dfrac{\pi}{2}-\theta<\theta'<\dfrac{\pi}{2}+\theta\\ -1, & \dfrac{\pi}{2}+\theta\leqslant\theta'\leqslant\pi\end{cases}$$

From this equation and Eq. (3a), Eq. (18) becomes

$$\beta(\mu)=(2\pi)^{-1}\int_{\pi/2-\theta}^{\pi/2+\theta}\cos^{-1}(\mathrm{ctn}\theta\ \mathrm{ctn}\theta')P(\cos\theta')\sin\theta'd\theta'+\frac{1}{2}\int_{\pi/2+\theta}^{\pi}P(\cos\theta')\sin\theta'd\theta'. \tag{22}$$

This gives $\beta(\mu)$ as single integrals over the phase function.

While at first we thought Eq. (22) was new, not having seen it in any of the more recent literature, the historical survey for Table 1 revealed that Dietzius (1922) gave Eq. (22) to within a constant factor. He gave no derivation, but J. A. Coakley (private communication) has shown that Eq. (22) follows from purely geometrical reasoning about the backscattering, which is probably how Dietzius got it. Nevertheless, our purely analytic derivation is new, and indeed becomes, to the best of our knowledge, the only extant derivation of Eq. (22) in the literature.

Note that the backscattered fraction for monodirectional radiation incident from directly overhead follows easily from Eq. (22), and is

$$\beta(1)=\frac{1}{2}\int_{\pi/2}^{\pi}P(\cos\theta)\sin\theta d\theta. \tag{23}$$

We can also calculate the backscattered fraction for grazing illumination, $\beta(0)=\frac{1}{2}$, from Eq. (22). The isotropic scattering limit, $\beta(\mu)=\frac{1}{2}$, is obtained straightforwardly from Eq. (5).

Eq. (22) presents the same problem with respect to numerical integration that Eq. (15a) for $\bar{\beta}$ did, namely the integrand in the first term has cusps at the endpoints of the interval of integration. However, by making the change of variable

$$\zeta=\cos^{-1}(\mathrm{ctn}\theta\ \mathrm{ctn}\theta'),$$

Eq. (22) becomes

$$\beta(\mu)=(2\pi)^{-1}\int_{\zeta=0}^{\zeta=\pi}\zeta P[\mu_\theta(\zeta)]d[-\mu_\theta(\zeta)]+\frac{1}{2}\int_{-1}^{-\sin\theta}P(\mu')d\mu', \tag{24}$$

where

$$\mu_\theta(\zeta)\equiv\frac{\cos\zeta}{(\cos^2\zeta+\mathrm{ctn}^2\theta)^{\frac{1}{2}}}.$$

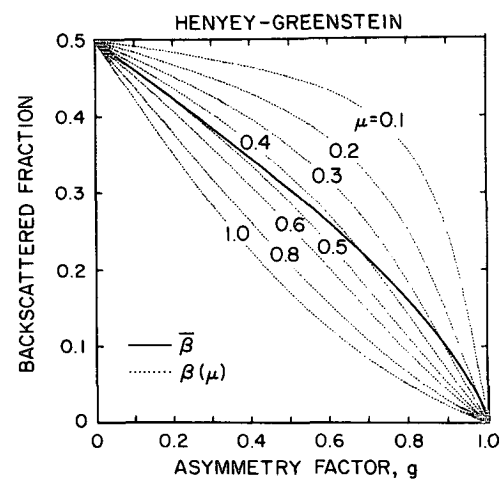

FIG. 3. Backscattered fractions $\bar{\beta}$ and $\beta(\mu)$ for the Henyey–Greenstein phase function versus the asymmetry factor g for a range of values of μ.

The integrands in Eq. (24) have no cusps or other bad behavior.

For the Henyey–Greenstein phase function (16), $\beta(\mu)$ can be expressed, after integrating Eq. (24) by parts, in terms of complete elliptic integrals of the third kind (see, e.g., Hancock, 1958, Chap. 19). But the expression is complicated and we have therefore omitted it, especially since numerical integration directly from Eq. (24) may be more efficient. However, we have plotted $\beta_{\rm HG}(\mu)$ and $\bar{\beta}_{\rm HG}$ as a function of g in Fig. 3 for several values of μ. Figure 3 illustrates the difficulty of selecting a "global mean zenith angle" for the purpose of estimating the backscattered fraction $\bar{\beta}$. A value of 60° ($\mu=\frac{1}{2}$), the mean value of the solar zenith angle over the sunlit earth, is often suggested. Indeed, the $\bar{\beta}$ and $\beta(\frac{1}{2})$ curves virtually coincide for $g\leqslant 0.3$; but as g increases, so does the appropriate "mean angle." For $g=0.7$ it would be about 67° ($\mu=0.4$), the value used by Dietzius (1922), Albrecht (1933) and Hewson (1943); for $g=0.9$ it would be about 73° ($\mu=0.3$). Fig. 3, of course, refers only to the Henyey–Greenstein phase function, but we expect that it is representative for the earth's atmosphere (based in part on our considerations in Section 5).

4. Values of $\bar{\beta}$, $\beta(\frac{1}{2})$ and $\beta(1)$ for spherical particles

In Fig. 4 we plot $\bar{\beta}$, $\beta(\frac{1}{2})$ and $\beta(1)$ versus the Mie size parameter $x=2\pi r/\lambda$ (where r is particle radius and λ wavelength) for a range of values of the imaginary index of refraction from 0 to 1.0. This range of imaginary index brackets almost any aerosol which one is likely to find in the earth's atmosphere (indeed, imaginary indices >0.1 are rare in the solar spectrum, although values up to 1.0 are possible for soot and other industrial pollution material). The real part of the index of refraction has been taken equal to 1.5 in Fig. 4 and subsequent figures, which is typical for *dry* atmospheric aerosol; however, our conclusions below are unaltered by realistic variations in the real index. In particular, we obtained very similar results when it was set equal to 1.335.

The behavior of the curves in Fig. 4 as functions of Mie size parameter and imaginary index is well understood (cf. Hansen and Travis, 1974). The point we wish to make from Fig. 4 is, however, that

$$\bar{\beta}\geqslant\beta(\tfrac{1}{2})\geqslant\beta(1). \tag{25}$$

These inequalities hold for all values of Mie size parameter and refractive index as long as $g\geqslant 0$ (if $g<0$,

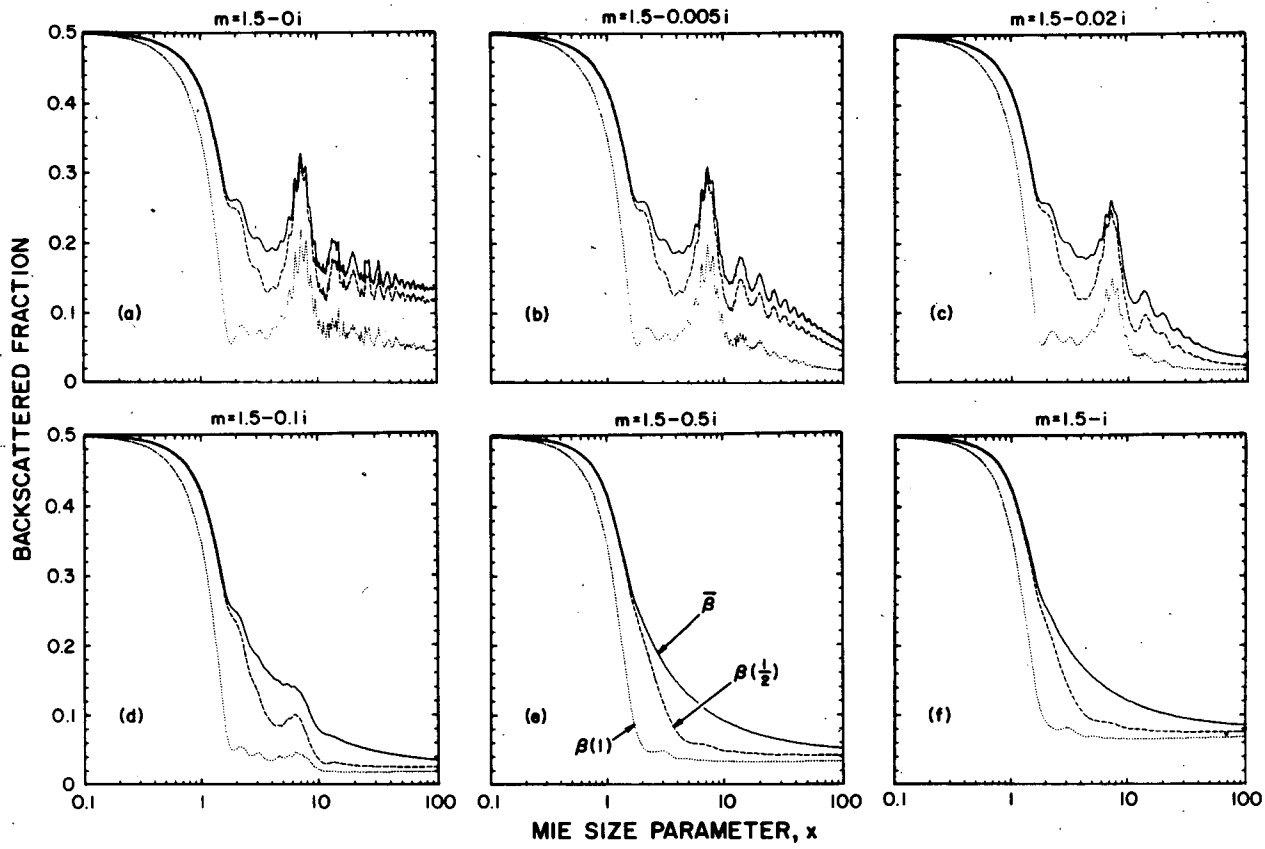

FIG. 4. Backscattered fractions $\bar{\beta}$, $\beta(1)$ and $\beta(\frac{1}{2})$ versus the Mie size parameter x for real refractive index of 1.5 and a range of imaginary indices.

as in small, highly reflective particles, the inequalities would be reversed). The inequalities can be observed in Fig. 3 as well, for the Henyey–Greenstein phase function. Hence we conjecture that (25) always holds for phase functions typical of the earth's atmosphere; but in spite of the formal similarity of Eqs. (15b) and (24), we have been unable to establish this result rigorously. We suspect that the general shape of atmospheric phase functions—large for small angles of scattering, generally declining as the scattering angle increases—plays an important role in maintaining (25). It can, in fact, be shown[2] that $\bar{\beta} \geqslant \beta(1)$ for phase functions satisfying

$$P(\cos\theta) \leqslant P[\cos(\pi-\theta)] \quad \text{for} \quad \frac{\pi}{2} \leqslant \theta \leqslant \pi, \qquad (26)$$

which is true for most if not all atmospheric phase functions. Eq. (15b) can be rewritten as

$$\bar{\beta} = \frac{1}{2}\int_{\pi/2}^{\pi}\left[\frac{(\pi-\theta)}{\pi}P[\cos(\pi-\theta)] + \frac{\theta}{\pi}P(\cos\theta)\right]\sin\theta d\theta. \qquad (27)$$

Using the inequality (26), it thereby follows that the integrand of Eq. (27) is everywhere greater than the integrand of Eq. (23).

Hence both $\beta(\frac{1}{2})$ and $\beta(1)$ are *systematic* underestimates of the globally averaged backscattering $\bar{\beta}$. No amount of averaging over particle size distribution, wavelength, optical properties, etc., is going to alter this state of affairs. $\beta(1)$ cannot even be called an approximation to $\bar{\beta}$, since it underestimates $\bar{\beta}$ by a factor of 2–3 almost everywhere. $\beta(\frac{1}{2})$ typically underestimates $\bar{\beta}$ by about 0.03 and never by more than 0.06, so it may be a satisfactory approximation in some circumstances. But using Eq. (15b), it will now be less difficult to calculate $\bar{\beta}$ than it had been to calculate $\beta(\frac{1}{2})$.

5. $\bar{\beta}$ as a function of g

As we noted in the Introduction, the well-known Sagan–Pollack approximation is based on relating the backscattered fraction to the asymmetry factor g [Eq. (7)]. There are several reasons for being interested in such a relationship. First, the two simplest approximations in radiative transfer, the Eddington (see, e.g., Shettle and Weinman, 1970; Joseph *et al.*, 1976) and the two-stream, are formulated in terms of g and of $\bar{\beta}$ and $\beta(\mu)$, respectively. Only by discovering the relationships between $\bar{\beta}$, $\beta(\mu)$ and g can we build a bridge between these two approximations, and thereby discern their essential interrelation. Second, van de Hulst (1974) has emphasized that $g(=\omega_1/3)$ is the fundamental phase function parameter for radiative transfer, and that the influence of the higher coefficients $(\omega_2, \cdots)$ in the phase function expansion (11) is weak unless single scattering dominates. Thus, it is of intrinsic interest to relate any other phase function parameter—such as $\bar{\beta}$—to g. Third, $\bar{\beta}$ and $\beta(\mu)$ have a more direct physical interpretation than g in terms of thin-layer albedos (Eqs. 9 and 10), and thus are simpler to measure. It would be highly desirable to estimate g directly from such measurements.

We shall examine three expressions relating $\bar{\beta}$ and g. One is $\bar{\beta}_{\rm HG}(g)$ [Eq. 17], derived for the Henyey–Greenstein phase function. The other two formulas are linear in g: the first is the Sagan–Pollack expression (7), $\frac{1}{2}(1-g)$, and the second involves the first two terms of the series (12) for $\bar{\beta}$, $\frac{1}{2}(1-\frac{3}{4}g)$. (Actually, the Sagan–Pollack expression is a two-term expansion of the Chandrasekhar backscattered fraction β_c.) In Fig. 5, $\bar{\beta}, \bar{\beta}_{\rm HG}(g), \frac{1}{2}(1-g)$ and $\frac{1}{2}(1-\frac{3}{4}g)$ are plotted as a function of the Mie size parameter x, for the same set of imaginary indices of refraction as in Fig. 4. We observe that $\frac{1}{2}(1-g)$ and $\frac{1}{2}(1-\frac{3}{4}g)$ are lower and upper bounds, respectively, for $\bar{\beta}$:

$$\tfrac{1}{2}(1-g) \leqslant \bar{\beta} \leqslant \tfrac{1}{2}(1-\tfrac{3}{4}g) \quad \text{for} \quad g \geqslant 0. \qquad (28)$$

Indeed, these seem to be, based on a large sample of cases, only a few of which are shown here, the *best possible* linear-in-g bounds for $\bar{\beta}$. The arithmetic mean of the two bounds, $\frac{1}{2}(1-\frac{7}{8}g)$, approximates $\bar{\beta}$ with an error no worse than $g/16$ for all g. We also note that (28) holds rigorously for Henyey–Greenstein phase functions. As before, the inequalities in (28) must be reversed if $g<0$.

Fig. 5 further shows that $\bar{\beta}_{\rm HG}(g)$ is an excellent approximation to $\bar{\beta}$; it differs from $\bar{\beta}$ by no more than 0.02 at any value of Mie size parameter when the imaginary index $n_{\rm im} \leqslant 0.1$. For $n_{\rm im}=0.5$ and $n_{\rm im}=1.0$ these maximum differences grow to 0.03 and 0.04, respectively; thus $\bar{\beta}_{\rm HG}$ deteriorates as an approximation to $\bar{\beta}$ for highly absorbing particles which are large with respect to the wavelength ($x \gg 1$), presumably because the Henyey–Greenstein phase function does not properly represent the more reflective nature of such particles. We note also that $\bar{\beta}_{\rm HG}(g)$ is always less than $\bar{\beta}$ for $x \leqslant 5$, roughly, and greater than $\bar{\beta}$ for $x > 5$. Thus in averaging over any reasonable size distribution of particles, there will be some cancellation of errors, and we have found that $\bar{\beta}_{\rm HG}(g)$ for specific size distributions almost always approximates $\bar{\beta}$ with an error of less than 0.01. We also suggest that the inverse of the relation $\bar{\beta}_{\rm HG}(g)$ will provide an excellent estimate of g if $\bar{\beta}$ is measured.

In Fig. 6 we have essentially taken $\bar{\beta}(x)$ and $g(x)$ and plotted them against each other rather than against x. In other words, each point on the solid "curves" represents $[g(x),\bar{\beta}(x)]$ for a particular x. The most remarkable thing about these curves is their erratic, zig-zag behavior, and the fact that $\bar{\beta}$ is often a *many-*

[2] We thank one of the reviewers for pointing out this proof.

valued function of g. It will thus never be possible to relate $\bar{\beta}$ and g in detail in terms of a single-valued function. We have found this multi-valued nature to persist even when one averages $\bar{\beta}$ and g over reasonable size distributions, although in that case the phenomenon is considerably mitigated. The multi-valuedness also gradually disappears as the absorbing power of the particle increases, and in fact is practically gone at $n_{\text{im}}=0.1$. Of course, both $\bar{\beta}$ and g are merely integral properties of the phase function, and so the phase function may vary in ways which hold g constant while $\bar{\beta}$ varies, and vice versa; and this is in fact what sometimes happens. That the multi-valuedness disappears as the absorbing power increases is to be expected, since the structure in the phase function, and therefore in $\bar{\beta}$ and g, is smoothed out as n_{im} increases.

As a final comment on the inequalities (28), we note that, as a consequence of Eqs. (8) and (15a), they may be written

$$\int_{\theta=0}^{\theta=\pi} \tfrac{1}{4}(1-\cos\theta)P(\mu)d\mu \leqslant \int_{\theta=0}^{\theta=\pi} \theta(2\pi)^{-1}P(\mu)d\mu \leqslant \int_{\theta=0}^{\theta=\pi} \tfrac{1}{4}(1-\tfrac{3}{4}\cos\theta)P(\mu)d\mu.$$

The functions weighting $P(\mu)$ in these integrals are plotted in Fig. 7. Since the preponderant part of $P(\mu)$ lies between $\theta=0°$ and $\theta=35°$ in the real atmosphere, the relationship in which these weighting functions stand to one another for $\theta\in[0°,35°]$ goes far toward explaining the inequalities (28). These inequalities are clearly not true for all $P(\mu)$ but are in reality artifacts of the shape of $P(\mu)$.

6. Thin-layer albedo for whole solar spectrum

Here we shall examine the effect of particle radius and imaginary refractive index on globally averaged albedo due to an optically thin, horizontally homogeneous scattering layer of spherical particles.

Let S_λ be the wavelength dependent solar flux (normal to its direction of propagation) at the top of the scattering layer. Then the thin-layer approximation [Eq. (9)] gives the reflected flux $F_\lambda^\uparrow$ for a particular solar zenith angle as

$$F_\lambda^\uparrow(\mu_0)=R_\lambda(\mu_0)\mu_0 S_\lambda=\omega_\lambda\beta_\lambda(\mu_0)\tau_\lambda S_\lambda.$$

This of course assumes no upwelling flux at the bottom of the scattering layer; in the presence of such a flux, the present results give, to first order, the *change* in the planetary albedo due to the scattering layer. Averaging

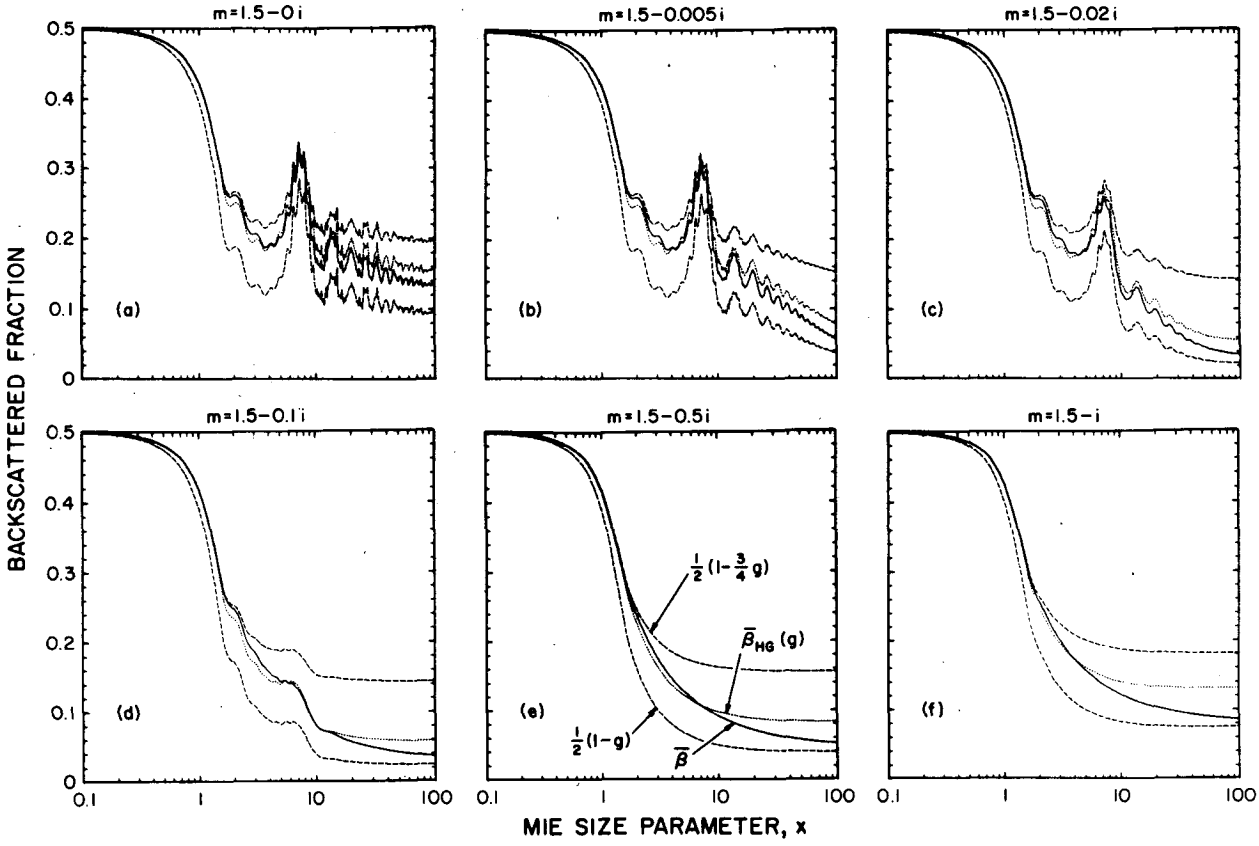

FIG. 5. Backscattered fraction $\bar{\beta}$ and the functions $\bar{\beta}_{HG}(g)$, $\frac{1}{2}(1-g)$ and $\frac{1}{2}(1-\frac{3}{4}g)$ [g=asymmetry factor] versus the Mie size parameter x for real refractive index of 1.5 and a range of imaginary indices.

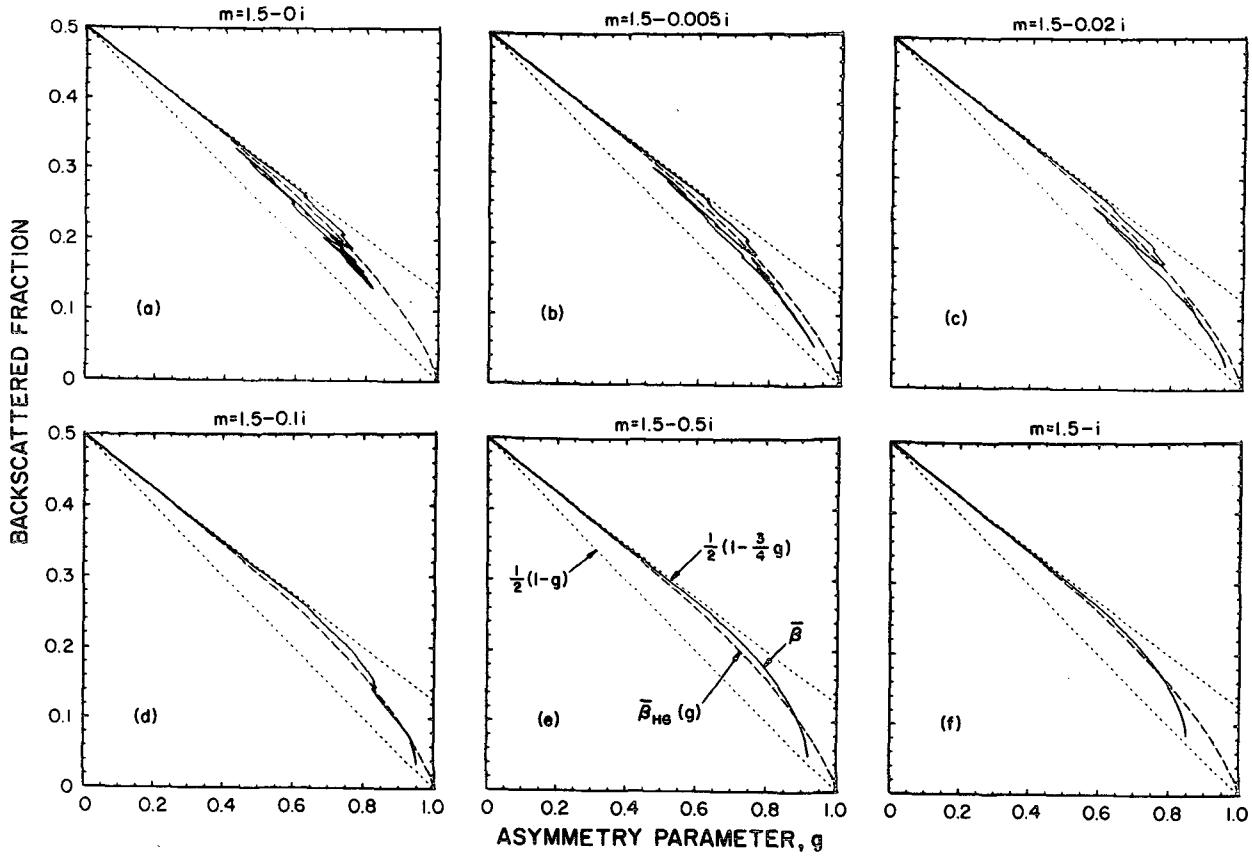

FIG. 6. Backscattered fraction $\bar{\beta}$ and also the functions $\bar{\beta}_{HG}(g)$, $\frac{1}{2}(1-g)$ and $\frac{1}{2}(1-\frac{3}{4}g)$ versus the asymmetry factor g for real refractive index of 1.5 and a range of imaginary indices.

over all solar zenith angles gives the "globally averaged albedo" at a particular wavelength:

$$\bar{R}_\lambda = \int_0^1 F_\lambda^\uparrow(\mu_0)d\mu_0 \Big/ \int_0^1 \mu_0 S_\lambda d\mu_0 = 2\omega_\lambda \bar{\beta}_\lambda \tau_\lambda$$

in consonance with Eq. (10). Integrating over the solar spectrum gives the planetary albedo

$$\bar{R} = \int_{0.3\,\mu m}^{3\,\mu m} \bar{R}_\lambda S_\lambda d\lambda \Big/ \int_{0.3\,\mu m}^{3\,\mu m} S_\lambda d\lambda. \qquad (29)$$

The 0.3 μm cutoff simulates ozone absorption.

Calculated values of $\bar{R}$ are presented in Fig. 8. We have, like Cadle and Grams (1975), fixed the *mass* concentration M of the scattering layer equal to 1 μg m^{-3}, so that the number concentration

$$N = \frac{3M}{4\pi r^3 d}$$

(d=particle density) varies, in Fig. 8, from 10^5 cm^{-3} at $r=0.01$ μm to 10^{-4} cm^{-3} at $r=10$ μm. We take the layer to be of thickness $\Delta Z=10$ km and assume the particles are of density $d=2$ g cm^{-3}. The only thing which recommends these particular values of M, d and ΔZ over any others is that they may be typical of a stratospheric aerosol layer. Because of linearity in optical depth, $\bar{R}$ scales linearly with ΔZ and M and inversely with d, so Fig. 8 is quite general in this respect.

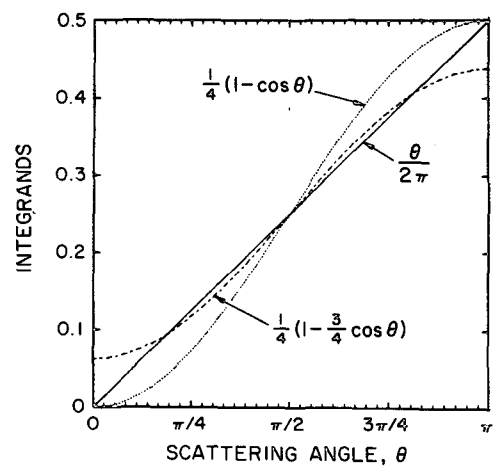

FIG. 7. Integrands $\theta/2\pi$, $\frac{1}{4}(1-\cos\theta)$ and $\frac{1}{4}(1-\frac{3}{4}\cos\theta)$ [arising from the integral form of inequality (28)] plotted versus θ.

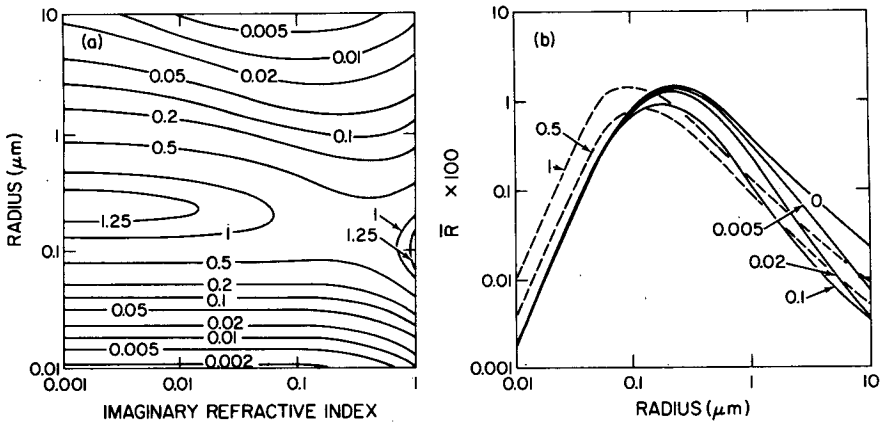

FIG. 8. Globally averaged, solar-spectrum albedo $\bar{R}(\times 100)$ for an optically thin layer of spherical particles of fixed mass concentration 1 μg m^{-3}, density 2 g cm^{-3} and thickness 10 km: (a) plotted as contours versus particle radius r and imaginary refractive index n_{im}; (b) plotted versus particle radius r for a range of imaginary indices. Real refractive index is 1.5 in both cases.

Values of $\bar{R}$ were computed for spherical particles with a real refractive index of 1.5 for large ranges of imaginary refractive index and particle radius. Thekaekara's (1973) values were used for S_λ, although Fig. 8 was barely altered if S_λ was approximated by a 6000 K blackbody. Indeed, Fig. 8 was affected only slightly when we set $S_\lambda = 0$ in the near-IR water vapor bands to simulate the effect of putting the aerosol layer lower down in the atmosphere (this procedure neglects the effect of Rayleigh scattering on S_λ, of course). The computed values of $\bar{R}$ are plotted in two different ways in Fig. 8: as contours of constant $\bar{R}(\times 100)$ in Fig. 8a and versus radius in Fig. 8b for the same selection of imaginary indices as in previous figures.

From both the contour plot and line drawing we observe that $\bar{R}$ is maximal ($\sim 1\%$) when all particles are roughly 0.2–0.3 μm in radius, as long as the imaginary index n_{im} is smaller than about 0.2. As n_{im} increases beyond 0.2, the maximal effect is produced by progressively smaller particles, until by $n_{im} = 1$, 0.08 μm particles are having the maximum effect on planetary albedo. When the particle size is held constant, other interesting effects on $\bar{R}$ are observed. For particles $\gtrsim 0.2$ μm radius, increasing n_{im} will tend to suppress some of their backscattering. After a certain point, however, the backscattering begins to increase with increasing absorption; this reversal occurs for n_{im} values in the range 0.1–0.5, depending on the particle size. The effect of particles < 0.1 μm radius on $\bar{R}$ is nearly independent of imaginary index for $n_{im} \lesssim 0.2$, as evidenced by the almost horizontal contours in the lower left side of Fig. 8a; but as n_{im} increases beyond 0.2, the backscattering effect of these small particles increases dramatically, which may be seen in the left-hand part of Fig. 8b. Thus, increasing the absorption of < 0.1 μm particles sufficiently far will always result in a larger planetary albedo than in the no-absorption case. It should be noted that this anomalous behavior takes place for a size range of particles for which measurements are very poor and inconclusive.

7. Summary and conclusion

New formulas give the backscattered fractions $\bar{\beta}$ and $\beta(\mu)$ for isotropically and monodirectionally incident radiation, respectively, as single integrals over the scattering phase function. These quantities are normally defined as complicated multiple integrals over the phase function. Using the new formulas, it is shown that at least 70% of the value of $\bar{\beta}$ arises from the forward hemisphere of the phase function, where Mie theory is a good approximation even for nonspherical particles. Thus the effect of nonsphericity on backscatter may not, on the average, be of major importance.

Putting the Henyey–Greenstein phase function into one of the new formulas gives an approximation to $\bar{\beta}$ for spherical particles (in terms of the asymmetry factor g) which is very accurate over wide ranges of particle radius and refractive index. We conjecture that a similar procedure will lead to an approximation for $\beta(\mu)$ of comparable accuracy. Very tight empirical linear-in-g bounds for $\bar{\beta}$ are also discovered. The relationship between $\bar{\beta}$ and g for spherical particles is shown to be a multiple-valued one, so that Eddington and two-stream approximations can never be uniquely related.

Both $\beta(1)$ and $\beta(\frac{1}{2})$ (the former having been used in many climatic impact of aerosol studies, the latter being the "60° mean zenith angle approximation") are shown to systematically underestimate $\bar{\beta}$, very significantly so in the case of $\beta(1)$. The correct "mean zenith angle" for terrestrial aerosols will generally fall between 65° and 75° and will be a rather sensitive function of the phase function asymmetry factor.

For a uniform, optically thin aerosol layer of fixed mass concentration covering a planet, the greatest augmentation of planetary albedo will be caused by 0.2–0.3 μm particles if their imaginary refractive index is less than 0.2. For larger imaginary indices, the radius of the "maximal-effect" particles diminishes to about 0.08 μm. For particles <0.1 μm, the planetary albedo will actually be *enhanced* as their absorption increases, dramatically so as their imaginary index rises above 0.2. The latter effect is unlikely to be important for natural terrestrial aerosols, but might be for man-made aerosols or aerosols on other planets.

Acknowledgments. The authors would like to thank Dr. James Coakley for stimulating our investigations of these matters and Mr. Alberto Mugnai for able programming assistance.

REFERENCES

Albrecht, F., 1933: Theoretical investigations on the transformation of radiation in clouds. *Meteor. Z.*, **50**, 478–486.

Atwater, M., 1970: Planetary albedo changes due to aerosols. *Science*, **170**, 64–66.

Barrett, E., 1971: Depletion of short-wave irradiance at the ground by particles suspended in the atmosphere. *Solar Energy*, **13**, 323–337.

Cadle, R., and G. Grams, 1975: Stratospheric aerosol particles and their optical properties. *Rev. Geophys. Space Phys.*, **13**, 475–501.

Chandrasekhar, S., 1960: *Radiative Transfer*. Dover, 393 pp.

Charlson, R., and M. Pilat, 1969: Climate: The influence of aerosols. *J. Appl. Meteor.*, **8**, 1001–1002.

——, W. Porch, A. Waggoner and N. Ahlquist, 1974: Background aerosol light scattering characteristics: Nephelometric observations at Mauna Loa Observatory compared with results at other remote locations. *Tellus*, **26**, 345–360.

Chu, C., and S. Churchill, 1955: Numerical solution of problems in multiple scattering of electromagnetic radiation. *J. Phys. Chem.*, **59**, 855–863.

Chýlek, P., and J. Coakley, 1974: Aerosols and climate. *Science*, **183**, 75–77.

——, G. Grams and R. Pinnick, 1976: Light scattering by irregular randomly oriented particles. *Science*, **193**, 480–482.

——, ——, G. Smith and P. Russell, 1975: Hemispherical backscattering by aerosols. *J. Appl. Meteor.*, **14**, 380–387.

Coakley, J., and P. Chýlek, 1975: The two-stream approximation in radiative transfer: Including the angle of the incident radiation. *J. Atmos. Sci.*, **32**, 409–418.

Davis, P., and P. Rabinowitz, 1967: *Numerical Integration*. Blaisdell, 230 pp.

Dietzius, R., 1922: The transmissivity and albedo of fog and clouds. *Beitr. Phys. Atmos.*, **10**, 202–206.

Ensor, D., W. Porch, M. Pilat and R. Charlson, 1971: Influence of the atmospheric aerosol on albedo. *J. Appl. Meteor.*, **10**, 1303–1306.

Junge, C. E., 1963: *Air Chemistry and Radioactivity*. Academic Press, 382 pp.

Hancock, H., 1958: *Lectures on the Theory of Elliptic Functions*. Dover, 498 pp.

Hansen, J., 1969: Exact and approximate solutions for multiple scattering by cloudy and hazy planetary atmospheres. *J. Atmos. Sci.*, **26**, 478–487.

——, and L. Travis, 1974: Light scattering in planetary atmospheres. *Space Sci. Rev.*, **16**, 527–610.

Hewson, E., 1943: The reflection, absorption, and transmission of solar radiation by fog and cloud. *Quart. J. Roy. Meteor. Soc.*, **69**, 47–62.

Holland, A., and G. Gagne, 1970: The scattering of polarized light by polydisperse systems of irregular particles. *Appl. Opt.*, **9**, 1113–1121.

Irvine, W. M., 1968: Multiple scattering by large particles II. Optically thick layers. *Astrophys. J.*, **152**, 823–834.

Joseph, J., and N. Wolfson, 1975: The ratio of absorption to backscatter of solar radiation by aerosols during Khamsin conditions and effects on the radiation balance. *J. Appl. Meteor.*, **14**, 1389–1396.

Joseph, J., W. Wiscombe and J. Weinman, 1976: The delta-Eddington approximation for radiative fluxes. *J. Atmos., Sci.* **33**, 2452–2459.

Lettau, H., and K. Lettau, 1969: Shortwave radiation climatonomy. *Tellus*, **21**, 208–222.

Liou, K., 1973: A numerical experiment on Chandrasekhar's discrete-ordinate method for radiative transfer: Applications to cloudy and hazy atmospheres. *J. Atmos. Sci.*, **30**, 1303–1326.

Lyzenga, D., 1973: Note on the modified two-stream approximation of Sagan and Pollack. *Icarus*, **19**, 240–243.

Mangulis, V., 1965: *Handbook of Series for Scientists and Engineers*. Academic Press, 133 pp.

Mecke, R., 1921: On the scattering and diffraction of light by fog and clouds. *Ann. Phys.*, **65**, 257–273.

Mitchell, J. M.: The effect of aerosols on climate with special reference to temperature near the earth's surface. *J. Appl. Meteor.*, **10**, 703–714.

Neumann, J., and A. Cohen, 1972: Climatic effects of aerosol layers in relation to solar radiation. *J. Appl. Meteor.*, **11**, 651–657.

Rasool, S., and S. Schneider, 1971: Atmospheric carbon dioxide and aerosols: Effects of large increases on global climate. *Science*, **173**, 138–141.

Roach, W., 1961: Some aircraft observations of fluxes of solar radiation in the atmosphere. *Quart. J. Roy. Meteor. Soc.*, **87**, 346–363.

Robinson, G., 1963: Absorption of solar radiation by atmospheric aerosol, as revealed by measurements at the ground. *Arch. Meteor. Geophys. Bioklim.*, **B12**, 20–40.

Russell, P., and G. Grams, 1975: Application of soil dust optical properties in analytical models of climate change. *J. Appl. Meteor.*, **14**, 1037–1043.

Sagan, C., and J. Pollack, 1967: Anisotropic nonconservative scattering and the clouds of Venus. *J. Geophys. Res.*, **72**, 469–477.

Schneider, S., 1971: A comment on "Climate: The influence of aerosols." *J. Appl. Meteor.*, **10**, 840–841.

Sellers, W., 1973: A new global climatic model. *J. Appl. Meteor.*, **12**, 241–254.

Shettle, E., and J. Weinman, 1970: The transfer of solar irradiance through inhomogeneous turbid atmospheres evaluated by Eddington's approximation. *J. Atmos. Sci.*, **27**, 1048–1055.

Thekaekara, M., 1973: Solar energy outside the earth's atmosphere. *Solar Energy*, **14**, 109–127.

van de Hulst, H. C., 1974: Multiple scattering in cloud layers: some results. *Proc. UCLA Intern. Conf. Radiation and Remote Probing of the Atmosphere*, J. Kuriyan, Ed., Western Periodicals.